MODIS thermal emissive bands calibration improvements for Collection 7

Tiejun Chang[a], Ashish Shrestha[a], Carlos Perez Diaz[a], Na Chen[a], Aisheng Wu[a], Truman Wilson[a], Yonghong Li[a], and Xiaoxiong Xiong[b]

[a] Science Systems and Applications, Inc., Lanham, MD 20706
[b] Sciences and Exploration Directorate, NASA/GSFC, Greenbelt, MD 20771

Abstract

The MODIS thermal emissive bands (TEB) radiometric calibration uses a quadratic function for the instrument response, and the calibration coefficients look-up tables (LUTs) are updated using the response of an on-board blackbody (BB). After more than 21 and 19 years on-orbit, the TEB performances for Terra and Aqua MODIS have been generally stable. However, contamination from electronic crosstalk, a known issue since prelaunch, has affected the L1B image quality and measurement accuracy. In addition to the photovoltaic (PV) longwave infrared (LWIR) bands crosstalk correction included in Terra MODIS Collection 6.1 (C6.1), a crosstalk correction for select detectors in the Terra and Aqua mid-wave infrared (MWIR) and Aqua PV LWIR bands are applied in C7. The mission-long crosstalk coefficients for the selected detectors are derived and populated in the form of LUTs. The crosstalk correction is applied to both on-orbit calibration and the algorithm used to generate Earth-view L1B products. Among these detectors, the Aqua MODIS band 24 detector 1 crosstalk has the largest impact on image quality, with striping observed over cold scenes for both Terra and Aqua MODIS. The images of C7 L1B and C6.1 are compared to assess the impact of the correction. Additional assessments using Earth-view measurements and inter-comparison also revealed the need for improvement of calibration stability and consistence for select bands. Additional improvements for long-term stability and mirror side consistence were developed using quasi-deep convective clouds (qDCC), Dome-C, ocean, desert, and inter-comparison with other instruments.

Keywords: MODIS, radiometric calibration, TEB, crosstalk, calibration algorithm

1. INTRODUCTION

The Moderate Resolution Imaging Spectroradiometer (MODIS) is one of the key instruments aboard the NASA Earth Observing System Terra and Aqua satellites, launched in 1999 and 2002, respectively. Although the two MODIS instruments have exceeded their design life, they continue to operate nominally [1-4]. MODIS has provided continuous global observations and produced an unprecedented amount of science data products for studies of the Earth's land, ocean, and atmosphere[5-9]. MODIS has 36 spectral bands, where bands 1 to 19 and 26 are the reflective solar bands (RSB) covering a wavelength range from 0.41 to 2.1 μm, and bands 20 to 25 and 27 to 36 are the thermal emissive bands (TEB) with wavelengths ranging from 3.8 to 14.2 μm. For TEB, the blackbody (BB), along with lunar observations and Earth-view (EV) measurements, are used for post-launch calibration. The MODIS TEB on-orbit calibration, performed with an on-board BB and a space view (SV), uses a quadratic response function. The nonlinear calibration coefficients are characterized on-orbit with the quarterly-scheduled BB warm-up and cool-down (WUCD) events. During WUCD, the BB temperature varies from 270 K to 315 K. The instrument's non-linear coefficient and offset terms are updated (as needed) in the form of look-up tables (LUT) for the L1B product. Electronic crosstalk, identified during preflight characterization, has shown increased effects on-orbit, primarily on the image quality and radiometric stability[10,11]. In particular, the electronic crosstalk effects increased substantially in Terra MODIS post the safe-mode event in 2016 and subsequent mitigation strategies using lunar measurements have been developed and implemented[11].

Due to the challenges associated with the accurate determination of the offset coefficient in the response function using these on-orbit WUCD measurements, the Collection 6.1 (C6.1) algorithm handles the offset coefficient for each mirror side differently for Terra MODIS and continues to rely on pre-launch offset coefficients for the Aqua MODIS TEB except for bands 31 and 32. In this paper, we provide calibration algorithm improvements for the Collection 7 (C7) L1B product.

2. BACKGROUND

2.1 MODIS TEB calibration algorithm

MODIS TEB includes mid-wave infrared (MWIR) bands 20-25, covering a wavelength range from 3.8 to 4.5 μm, and long-wave infrared (LWIR) bands 27-36, from 6.8 to 14.2 μm. TEB detectors are located on two cold focal plane assemblies (CFPAs): a short-wave and mid-wave infrared (SMIR) FPA and a LWIR FPA. The two CFPAs are nominally controlled on-orbit at 83K using a passive radiative cooler and a heater. The on-board BB serves as the primary calibration source while the SV provides a reference for the instrument background. Normally, this temperature is set to 290 K and 285 K for Terra and Aqua MODIS, respectively. Starting in April 2020, the Terra BB temperature setpoint has been changed to 285 K. The MODIS TEB calibration uses a quadratic calibration algorithm on a scan-by-scan basis for each TEB detector and scan-mirror side. The linear gain coefficient of the response function is calibrated scan-by-scan using a two-point calibration performed via the response to the on-board BB referenced to the SV, and the non-linear and offset terms coming from an offline LUT that is updated periodically. The BB WUCD operation is used to characterize and update the instrument non-linear response coefficients on-orbit. Every WUCD operation is performed quarterly, and the BB temperature varies from instrument ambient temperature (about 270 K) to 315 K. The calibration radiance (L_{CAL}) from the BB view is defined as[12]:

$$L_{CAL} = RVS_{BB}\varepsilon_{BB}L_{BB} + (RVS_{SV} - RVS_{BB})L_{SM} + RVS_{BB}(1 - \varepsilon_{BB})\varepsilon_{cav}L_{cav}, \quad (1)$$

where ε is the BB or cavity (cav) emissivity, L is the radiance for the BB, scan mirror (SM), or cavity, and RVS is the response-versus-scan-angle at the SV or BB view. The TEB calibration is based on a quadratic algorithm that converts the digital response of the sensor to calibration radiance (L_{CAL}):

$$L_{CAL} = a_0 + b_1 dn_{BB} + a_2 dn_{BB}^2, \quad (2)$$

where a_0 and a_2 are the offset and non-linear coefficients, and dn_{BB} is the BB's digital response. Equations (1) and (2) are used for both the WUCD and scan-by-scan linear coefficient calibrations during nominal operation. The scan-by-scan linear coefficient, b_1, can be calculated using the emissivity, RVS, and nonlinear coefficients LUTs:

$$b_1 = [L_{CAL} - a_0 - a_2 dn_{BB}^2]/dn_{BB}. \quad (3)$$

Using the calibration coefficients for each detector and scan mirror side, EV radiance retrievals can be calculated by:

$$L_{EV} = \frac{1}{RVS_{EV}}[a_0 + b_1 dn_{EV} + a_2 dn_{EV}^2 - (RVS_{SV} - RVS_{EV})L_{SM}], \quad (4)$$

where RVS_{EV} is the EV RVS as a function of mirror incident angle. The TEB RVS come from pre-launch tests for Aqua MODIS and from post-launch using pitch maneuvers for Terra MODIS. A detailed description on the MODIS TEB calibration is described by Xiong et al[1].

2.2 MODIS TEB electronic crosstalk

Signal contamination in the form of electronic crosstalk has been observed in many of the TEB since pre-launch. This became particularly evident for Terra MODIS bands 27 − 30 after the instrument experienced a safe-mode event in February 2016, for which a correction was applied in C6.1 shortly after[10,11]. Moreover, some of the detectors in the Terra MODIS MWIR bands also show signs of electronic crosstalk contamination, which can be seen clearly from the Moon observations.

Generally, crosstalk occurs between bands and detectors that are located on the same FPA. The source of the contaminating signals can be identified using lunar data. There are two kinds of crosstalk. One is detector 1 contamination from detector 10 of a sending band. The second is band-to-band among MWIR bands or among photovoltaic (PV) LWIR bands. The contaminating signal has been assumed to be linearly proportional to the measured signal from the identified sending bands. Since electronic crosstalk affects the digital signal in each data sector, it will have an impact on the background signal as well as the signal from any measured EV or on-board calibrator (OBC) scene. However, since the background

contamination is at a nearly constant level, this contamination can be subtracted off with the rest of the background signal. In a simplistic fashion, the crosstalk coefficients, $c_{i,j}$, are in the form of a matrix which contains linear coefficient values that connect a detector's receiving contamination (i), to each of the detectors that send contamination (j). The correction is applied to the background-subtracted digital counts (dn) for each data sector in order to derive the calibration coefficients and EV scene radiance. Thus, the corrected signal on the pixel level can be written as:

$$dn_i(S,F) = dn_i^*(S,F) - \sum_j c_{i,j} dn_j^*(S,F+\Delta F_j) \quad (5)$$

Here, S and F represent the scan and frame numbers, respectively, ΔF_j is the relative frame offset of detector j with respect to detector i, and the * represents the digital counts before correction. A detailed description of the correction and its impact on the L1B data is described by Wilson et al.[11], and in the 2018 MODIS TEB electronic crosstalk workshop[13].

2.3 MODIS TEB Collection 6.1

The current MODIS C6.1 LUT on-orbit update algorithms for the Terra and Aqua MODIS TEB are summarized in Table 1 for Terra and Table 2 for Aqua [12,14]. The tables also include C7 calibration algorithms for comparison. The band 21 b_1 linear coefficient (not described in Table 1) is derived using the on-board BB cooldown (CD) data - with the offset and non-linear calibration terms constrained to zero in the fitting algorithm. The Terra MODIS photoconductive (PC) LWIR TEB crosstalk coefficients were derived using lunar observation analyses from the mission beginning. Moreover, an electronic crosstalk correction is applied to Terra MODIS PV LWIR bands 27-30 during calibration and Earth-view (EV) retrievals. The Aqua C6.1 MODIS TEB use the pre-launch a_0 with instrument temperature adjustment for PV bands and a_0=0 for PC bands and pre-launch adjusted a_2 calibration coefficients for all bands – except for bands 31 and 32 (a_0 is equal to zero and a_2 is derived using the CD data) [14]. In a general sense, the BT difference analyses between the current LUT and newly derived a_0 and a_2 calibration coefficients are performed to verify if a forward LUT update of the calibration algorithm coefficients is necessary. If the update criteria are exceeded, a LUT update is issued to meet the radiometric accuracy requirements of the L1B data in forward production.

Table 1. Terra MODIS C6.1 and C7 TEB calibration algorithms.

(PL: pre-launch; CD: cooldown)

Band	Terra C6.1		Terra C7	
	Calibration algorithm	Crosstalk correction (for calibration and EV)	Calibration algorithm	Crosstalk correction (for calibration and EV)
20	$a_{0\_ms1} = 0$ $a_{0\_ms2} = a_{0\_ms2}^{\text{free-fit}} - a_{0\_ms1}^{\text{free-fit}}$ CD a_2		Corrected a_0; CD a_2	Electronic cross-talk corrections for selected detectors
22			$a_{0\_ms1} = 0$ $a_{0\_ms2} = a_{0\_ms2}^{\text{free-fit}} - a_{0\_ms1}^{\text{free-fit}}$ CD a_2	
23				
24				
25				
27		PV LWIR electronic cross-talk		PV LWIR electronic cross-talk
28				
29			Corrected a_0; CD a_2	
30			MS Corrected a_0 CD a_2; Fixed after 003	
31	$a_0 = 0$ CD a_2		$a_0 = 0$ CD a_2	
32		PC LWIR optical cross-talk		PC LWIR optical cross-talk
33			Early mission: MS corrected a_0 Since 2003: $a_0 = 0$ CD a_2	
34				
35				
36				

Table 2. Aqua MODIS C6.1 and C7 TEB calibration algorithms.

Band	Aqua C6.1	Aqua C7	
	Calibration algorithm	Calibration algorithm	Crosstalk correction (for calibration and EV)
20 22-25	PL a_0 PL adjusted CD a_2 (CD: cooldown).	PL a_0 with MS correction CD a_2	Crosstalk corrections for selected detectors
27		PL a_0 with MS correction, CD a_2 No a_2 change after 2012036	Crosstalk corrections for all detectors
28			
29		PL a_0 with MS correction and Dome-C based correction, CD a_2 No a_2 change after 2012036	Crosstalk corrections for all detectors
30		PL a_0 with MS correction, CD a_2 No a_2 change after 2012036	
31, 32	a_0=0, CD a_2	Entire mission MS corrected a_0 CD a_2	
33-36	a_0=0 PL adjusted CD a_2		

3. TERRA MODIS TEB C7 CALIBRATION IMPROVEMENTS

Table 1 also lists the C7 calibration algorithm for Terra MODIS TEB. The major improvements include (1) MWIR bands crosstalk correction for selected detectors; (2) Early mission PC bands a_0 correction to reduce the mirror side difference; (3) Bands 20 and 29 a_0 correction and a_2 re-process to decrease cold scene bias; (4) Use of fixed a_0 and a_2 for band 30 to improve its calibration stability. Additional mirror side difference correction is also applied using the Dome-C and quasi-deep convective clouds (qDCC) analyses. This section presents these major improvements.

3.1 MWIR electronic crosstalk correction

A crosstalk correction for selected detectors of the Terra MWIR bands is applied in C7[13]. Each detector that was selected for correction underwent extensive evaluation of the correction's impact on the L1B product and image quality. Figure 1 displays the electronic crosstalk correction coefficients applied to the L1B product for selected detectors in the MWIR bands. Ultimately, it was decided that only 4 detectors (band 22 detector 8, band 23 detectors 1 and 10, and band 24 detector 1) in the Terra MWIR bands have contamination levels that are significant enough to require a correction in the L1B product. Figure 2 illustrates the L1B image quality improvement using the comparison before and after the crosstalk correction for band 24 detector1.

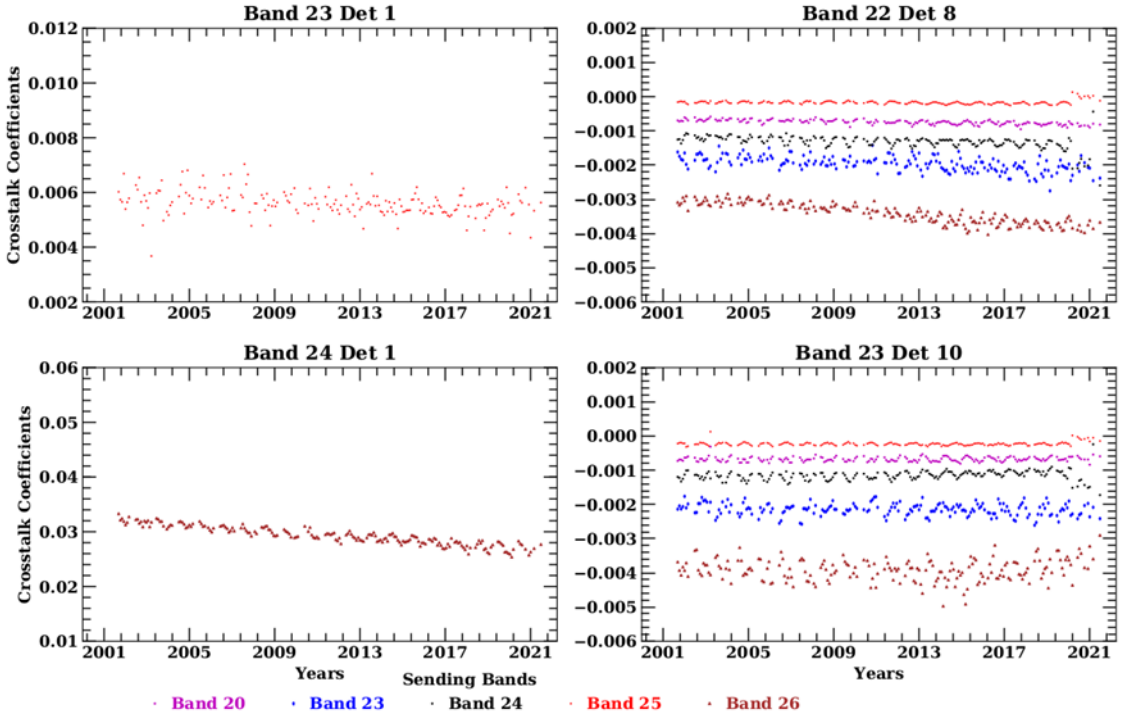

Figure 1. Terra MODIS C7 MWIR electronic crosstalk correction coefficients mission-long trends for the selected detectors and bands. The left two plots show the crosstalk coefficients trending for detector 1 of MWIR bands with sending signal from detector 10 of the sending band. The right two charts show the crosstalk coefficients for band 22 detector 8 and band 23 detector 10 with multiple sending bands.

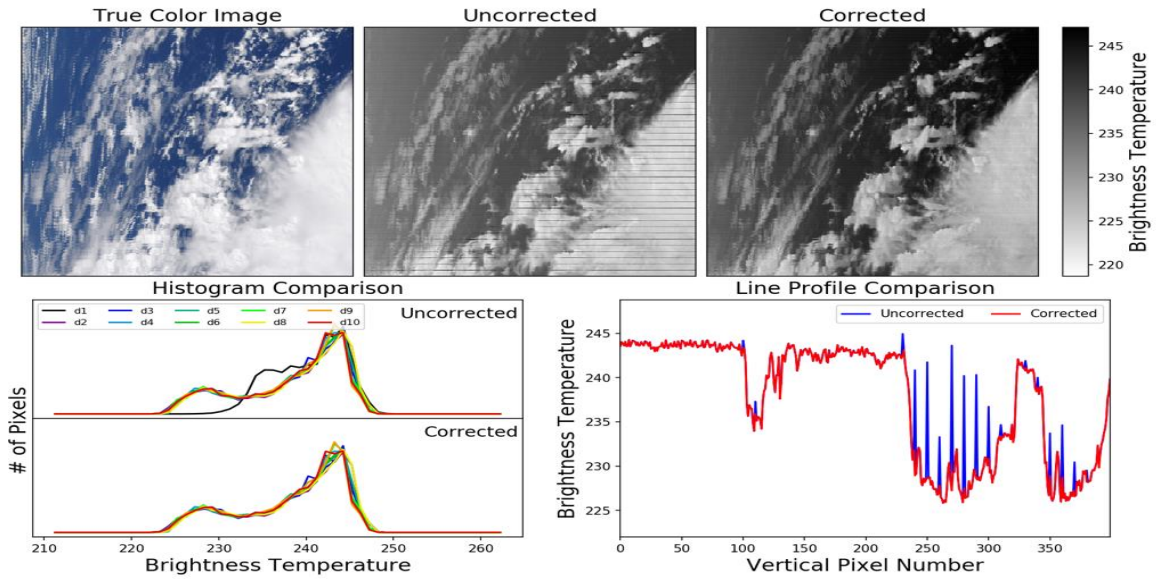

Figure 2. Crosstalk correction example for Terra MODIS band 24. (Top) True color, uncorrected, and corrected images. (Bottom left) Histogram comparisons for the selected scene before and after the electronic crosstalk correction is applied. (Bottom right) Vertical line profiles comparison through the center frame of the selected scene.

3.2 Nonlinear coefficient calibration improvement

3.2.1 Band 30 stability improvement

Inter-sensor comparisons and vicarious calibration approaches have confirmed that the Terra band 30 BTs from the C6.1 L1B have been drifting downward[15-19]. This has been observed both through the Terra MODIS - Infrared Atmospheric Sounding Interferometer (IASI) time series (2007-2019) [15] and MODIS mission-long EV trending results over qDCC, Dome Concordia (Dome-C), and the ocean trends[16-19], as shown in Figure 3. These biases are larger for scenes with lower BTs. To correct this artifact, for both the Dome-C site and an ocean location in the Bahamas, EV nadir measurement data for every year of the Terra MODIS mission was re-processed using the a_0 and a_2 calibration coefficients from a timestamp in 2003 that corresponds to the instrument's last major configuration change. Comparison tests between these coefficients and C6.1 demonstrated significant reduction in bias for both Earth scenes. Figure 4 illustrates the C7 bias corrections for the Dome-C and ocean targets. Thus, Terra MODIS C7 will use the a_0 and a_2 calibration coefficients from the 2003 LUT (after last configuration change) to re-process Terra MODIS band 30 for the instrument's entire mission. Moreover, the Dome-C, ocean, and qDCC Earth scenes will continue to be monitored for possible changes in C7.

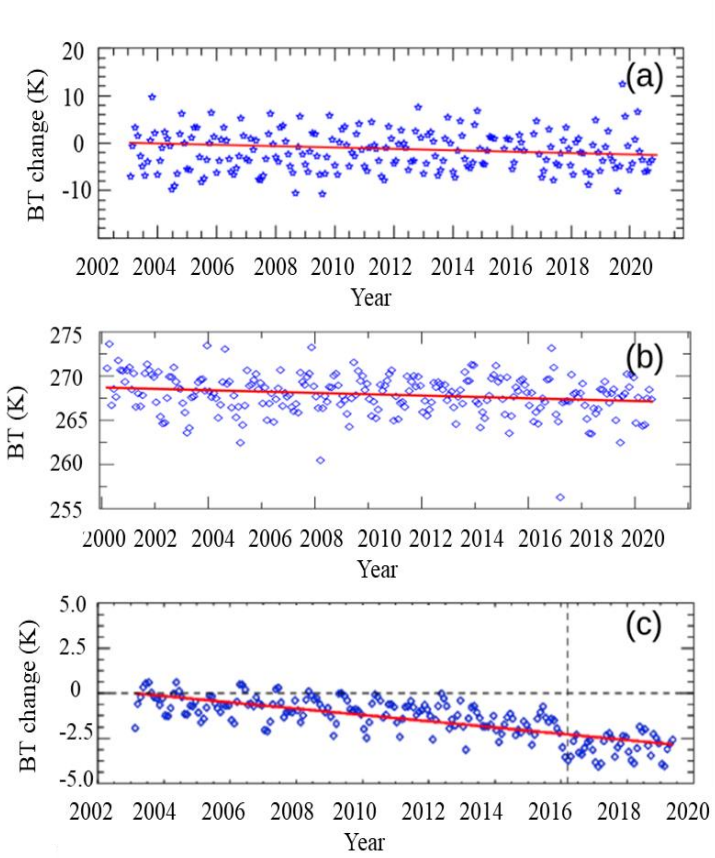

Figure 3. (a) Terra MODIS C6.1 band 30 BT relative to band 31 over Dome-C. (b) Terra MODIS C6.1 band 30 BT over the ocean. (c) Terra MODIS C6.1 band 30 BT relative to band 31 over qDCC. Blue markers represent monthly-averaged data. Red lines define the data's fit.

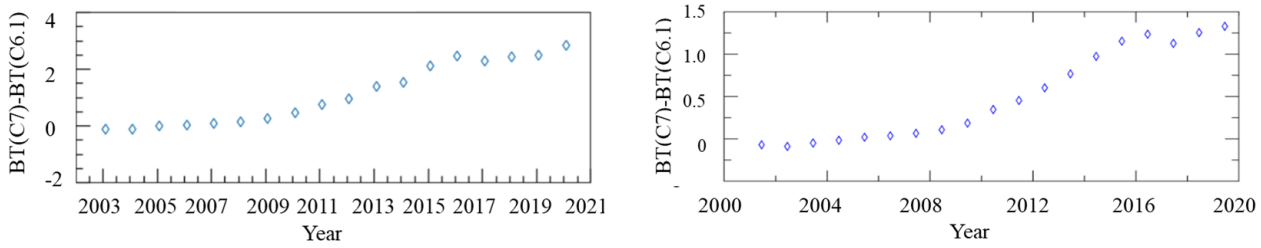

Figure 4. Terra MODIS C7 band 30 bias corrections (compared to C6.1) for the (left) Dome-C and (right) ocean targets. Blue markers represent monthly-averaged data.

The C7 L1B BT trends for Dome-C shows residual difference between mirror sides and drift in the EV time series. An algorithm for an additional a_0 correction was developed to reduce the mirror side difference. From the Dome-C residual mirror side difference assessment, additional time-dependent a_0 corrections are calculated. To preserve the mirror side consistency, this a_0 correction is applied to mirror side 1. The mirror side difference is assessed using measurements over Dome-C. Figure 5 shows Terra MODIS band 30 mirror side difference for C7 and C6.1 The mirror side difference is greatly reduced after the correction. Terra band 30 mission-long trending is assessed and compared between C6.1 and C7 using Dome-C and desert measurements. The left chart in Figure 5 shows the comparison of Dome-C trending for C6.1 and C7. The drift seen in C6.1 is mostly corrected in C7. The larger oscillation for the desert data is due to large seasonal BT fluctuations. A slight overcorrection remains and it will be continually monitored.

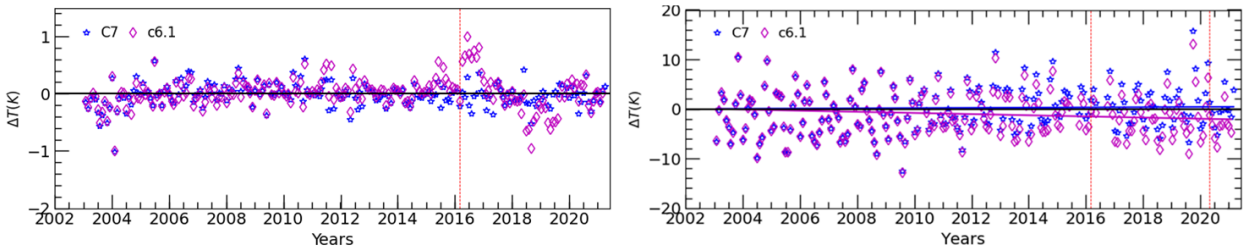

Figure 5. (Left) Terra MODIS band 30 mirror side difference in C6.1 and in C7 with additional a_0 correction. (Right) The comparison of Dome-C trending for C6.1 and C7 for Terra band 30.

3.2.2 Bands 20 and 29 cold scene bias correction

When compared to the IASI instrument, part of the payload of the MetOp series of polar-orbiting meteorological satellites, Terra MODIS has shown cold scene biases for some TEB, as demonstrated by Moeller et al.[15]. This has been further confirmed by MCST in separate efforts[16]. For band 20, warm scenes show quite stable trends. However, band 29 shows a slight upward trend for the warmer scenes. In order to mitigate these biases, a strategy combining the bias and drift analysis is used, where the BT-dependent biases are estimated using the Terra MODIS-IASI difference from 2007-2019, and the trends of the biases are obtained from MODIS retrievals over qDCC. Figure 6 illustrates the Terra MODIS mission-long retrievals over qDCC, Terra-IASI biases adjusted qDCC trending, and a_0 corrections for bands 20 and 29. Using the MODIS observations over qDCC referenced to the Terra-IASI biases, an a_0 correction is derived for each month of data. This a_0 correction, as well as the free-fitted a_2, are calculated using a yearly-averaged sliding window. Because Terra MODIS underwent several configurations and settings changes from the years 2000 to 2003, the average a_0 correction from 2003-2004 is used for band 20 over this early mission period to avoid discontinuity. Moreover, after every WUCD operation, an a_0 correction is applied to both mirror sides and a_2 is computed.

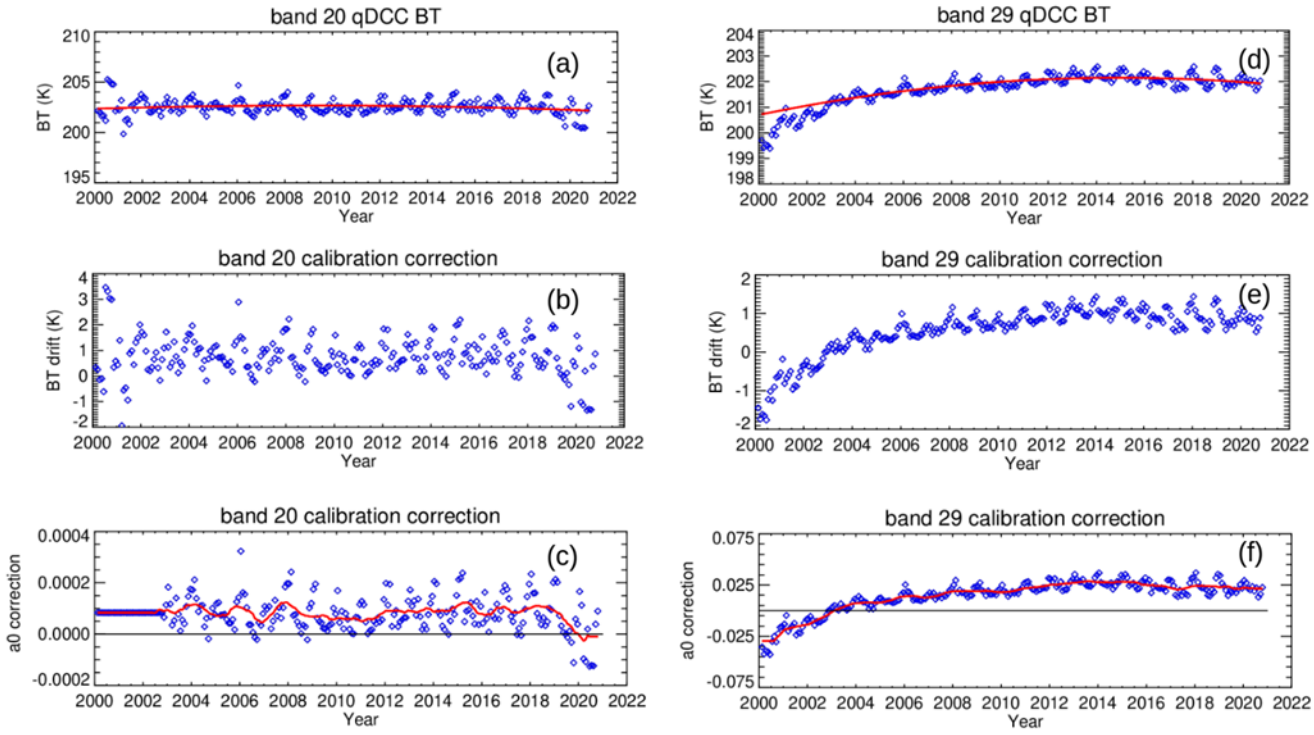

Figure 6. Terra MODIS mission-long retrievals over qDCC (a and d), Terra-IASI biases over qDCC (b and e), and a_0 correction (c and f) for bands 20 and 29. Blue markers represent monthly-averaged data. Red lines define data's fit in (a) and (d) and yearly moving average in (c) and (f).

3.2.3 Early mission PC bands mirror side difference correction

Early in the Terra MODIS mission (2000-2002), the instrument underwent several instrument setting and electronic configuration changes (Table 3). The instrument response was affected after each change and, consequently, the calibration data shows relatively larger uncertainty when compared to that after the year 2003. The mirror side differences were analyzed for each TEB during each time interval between these changes, and assessments over qDCC and Dome-C show relatively large (specify a number X BT (K)) mirror side differences and discontinuities for low BT measurements. MCST performed several analyses and found that re-processing the C7 LUTs to accommodate for new timestamps - more representative of each setting and configuration change - improves the calibration consistency and accuracy by generating LUTs for each change period. The PV bands mirror side differences were mostly reduced to within X K. However, because a_0 is set to zero for both mirror sides for the PC bands, residual mirror side differences remain. Figure 7 illustrates the Terra MODIS early mission mirror side BT differences for bands 34 (~0.5 K) and 36 (~0.8 K). Thus, MCST analyzed the mirror side BT differences using cold scenes and derived an a_0 correction associated with the mirror side differences for PC bands 33-36. This a_0 correction is used to generate the C7 a_0 and a_2 LUTs between 2000 and 2003. The test results show the correction of the mirror side difference using C7 LUT.

Table 3. Key Terra MODIS setting and configuration changes from 2000 to 2002.

Date	Changes
06/08/00	Cold focal plane assembly stopped controlling temperature
10/30/00	MODIS switches to B-side electronics configuration
07/02/01	MODIS switches to A-side electronics configuration using PS1
03/19/02	Spacecraft safe mode anomaly during maneuver
09/17/02	Switch to B-side formatter; other components remain on A-side

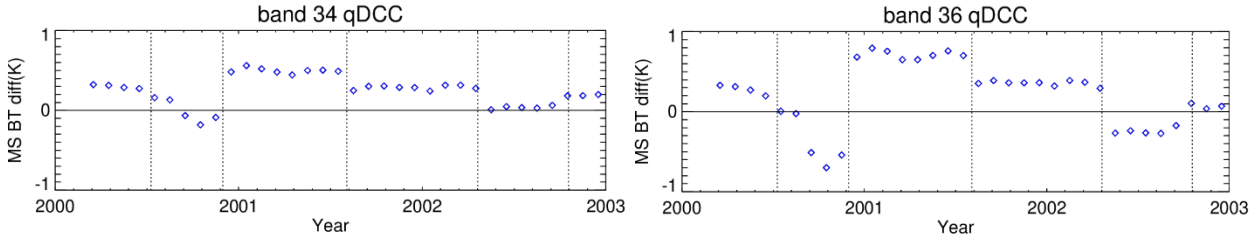

(a) (b)

Figure 7. Terra MODIS C6.1 early mission mirror side BT differences for bands (a) 34 and (b) 36. Blue markers represent monthly-averaged data.

3.2.4 Impact assessment

The impact on the L1B product due to the calibration algorithm improvement can be estimated using simulated L1A data. The BT measurement value for each band at different radiance levels can be calculated using C7 a_0 and a_2 LUTs and C6.1 LUTs. The differences of the BT at EV are calculated for each band and for different years. Table 4 summarizes the C7 impact assessment at three radiance levels for years 2005, 2016, and 2020. This assessment is for band-averaged data. The band 21 maximum radiance level is beyond the simulated digital response range, and it is not considered. As expected, the largest change observed is for band 30, which is up to 3K for most recent years at low BTs. The band 30 change is also time dependent since a major C7 improvement is mitigation of its downward trend. Bands 20 and 29 C7 calibration improvements are for low BT scenes.

Table 4. Terra MODIS TEB C7 impact assessments calculated as the BT difference between C7 and C6.1 in Kevin.

Year	2005			2016			2020		
Radiance level	0.3Ltyp	Ltyp	Lmax	0.3Ltyp	Ltyp	Lmax	0.3Ltyp	Ltyp	Lmax
20	-0.005	-0.002	-0.044	-0.002	-0.003	-0.032	-0.001	0.000	0.001
21	0.075	0.096	N/A	0.136	0.168	N/A	0.000	0.000	N/A
22	-0.002	0.002	0.013	0.001	-0.001	0.114	-0.002	0.002	0.034
23	0.001	-0.001	-0.006	0.004	-0.003	-0.014	0.000	0.000	-0.004
24	0.015	0.003	0.002	0.013	0.003	0.002	0.000	0.000	0.000
25	0.003	0.001	0.000	0.006	0.002	0.001	0.000	0.000	0.000
27	0.008	-0.005	-0.005	-0.300	-0.043	0.017	0.004	0.003	0.002
28	-0.024	-0.016	-0.008	-0.079	0.013	0.016	-0.007	-0.007	-0.003
29	-0.037	0.000	-0.013	-0.096	-0.022	-0.136	-0.133	0.008	0.003
30	0.042	0.061	0.037	2.402	2.079	1.049	3.072	2.666	1.318
31	-0.031	0.012	0.050	0.019	-0.008	-0.031	0.000	0.000	0.000
32	-0.036	0.013	0.056	0.021	-0.008	-0.032	0.000	0.000	0.000
33	-0.041	-0.027	-0.006	0.023	0.015	0.003	0.000	0.000	0.000
34	-0.041	-0.032	-0.022	0.022	0.017	0.011	0.000	0.000	0.000
35	-0.033	-0.029	-0.021	0.017	0.015	0.011	0.000	0.000	0.000
36	-0.024	-0.028	-0.026	0.019	0.018	0.016	0.000	0.000	0.000

3.2.5 Uncertainty update

The MODIS L1B product uncertainty algorithm is summarized and presented in previous literature by Xiong, et. al[20]. The calibration uncertainties propagate to the total uncertainty of the L1B product. The uncertainty comes from the calibration coefficients, calibration radiance source uncertainty, spectral uncertainty, digital response noise, and crosstalk uncertainty. The crosstalk contamination of the selected detectors and bands will contribute the uncertainty. A penalty LUT is prepared for the calculation of the crosstalk related uncertainty. The uncertainty is calculated for each pixel in L1B data as

uncertainty index. It includes the noise in the digital response of EV radiance and crosstalk effect, which are L1B measurement data related. Figure 8 shows the uncertainty, without EV noise and crosstalk effect, for TEB for selected years for C6.1 and C7. The major change from C6.1 to C7 is for the PV LWIR bands. The uncertainties for recent years are higher for these bands, especially for bands 27 and 30. These two bands have been affected by the larger contamination due to crosstalk and long-term stability issues. For C7, due to the calibration algorithm improvements and the LUT procedure update to follow the instrument response change, they are below the specification. Terra MODIS band 36 detectors are noisy ;hence the uncertainty is above the specification in both C6.1 and C7. Band 21 is a low gain band for fire detection and uses a linear calibration algorithm. The uncertainty is not shown in this chart.

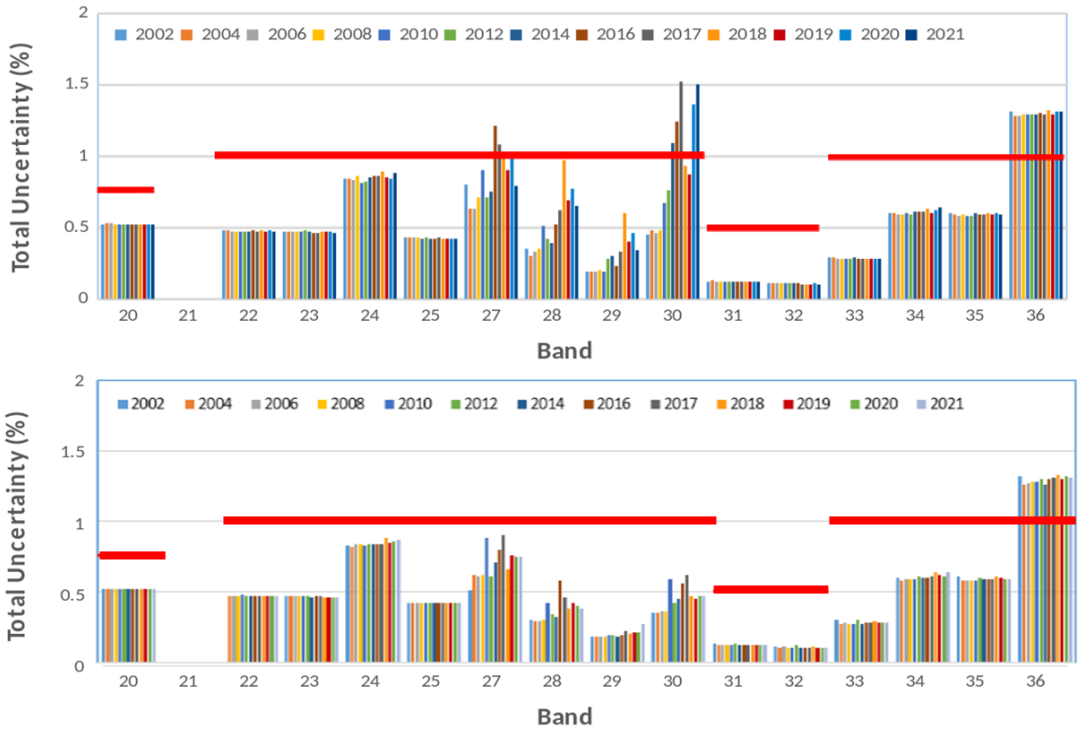

Figure 8. (Top) Terra MODIS TEB C6.1 uncertainty for selected years. (Bottom) Terra MODIS TEB C7 uncertainty for selected years. The red horizontal lines are the specifications.

4. AQUA MODIS TEB CALIBRATION IMPROVEMENTS

Table 2 in section 2.3 also lists the C7 calibration algorithm for Aqua MODIS TEB including (1) MWIR and LWIR bands crosstalk correction for select detectors; (2) Mission-long a_0 correction using qDCC and a_2 update using BB CD data to reduce the mirror side difference; and (3) PV LWIR bands nonlinear response calibration improvement to stability improvements. This section presents discusses these major improvements in detail.

4.1 Electronic crosstalk correction

Aqua MODIS C7 will introduce electronic crosstalk correction for the PV LWIR bands (except band 28) and for select detectors in the MWIR bands. Signatures of electronic crosstalk contamination are seen in lunar images by various Aqua MODIS bands from both the MWIR and LWIR FPAs. The lunar images from scheduled lunar observations are used to determine all the bands and detectors affected by electronic crosstalk artifacts including their respective sending bands and detectors. Moreover, linear crosstalk correction coefficients were derived from Moon observations for the pertinent

bands/detectors over the entire mission. Afterwards, these were used to generate corrected L1B images and to assess the impacts of electronic crosstalk on the calibrated imagery. A detailed description of the correction and its impact on the L1B data is described by Keller et al.[21,22].

4.1.1 MWIR electronic crosstalk correction

After various analyses and tests on the electronic crosstalk correction impacts on the L1B product, MCST proposes to apply electronic crosstalk corrections to select detectors in the Aqua MWIR bands. The electronic crosstalk corrections are applied to detector 1 (product order (P.O.)) for all MWIR bands except band 21. Figure 9 illustrates the Aqua MODIS C7 MWIR bands electronic crosstalk correction coefficients mission-long trends for selected detectors and bands, respectively. Generally, all coefficients are stable throughout the entire Aqua MODIS mission. Figures 10 shows example of the application of the electronic crosstalk correction coefficients to the L1B product for band 24. The L1B images displayed correspond to the granules from October 11th, 2019. It can be inferred from the images, BT profiles, and BT histograms that the application of the electronic crosstalk coefficients effectively removes striping and brings detector 1 in-family with the other detectors for all bands (more apparent for band 24, whose electronic crosstalk coefficients are larger (~4%) than for the other bands (<2%)).

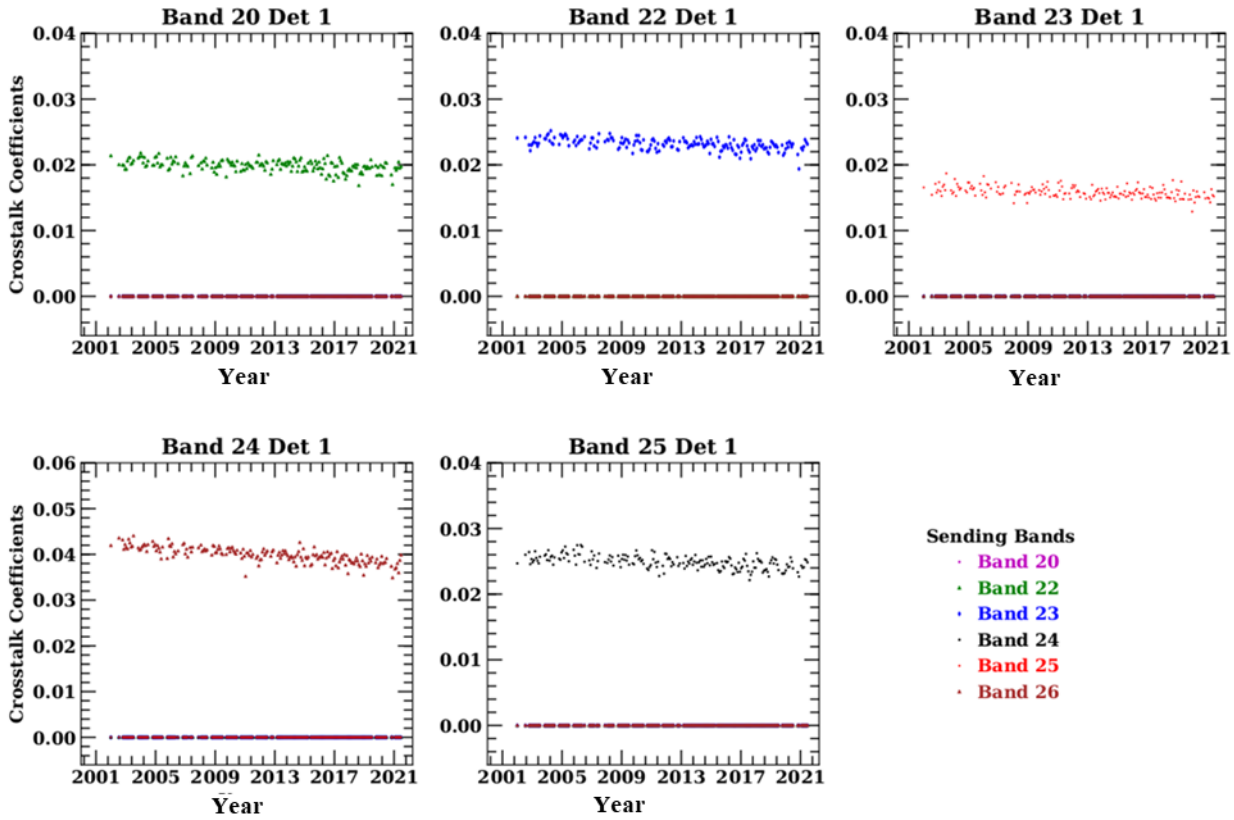

Figure 9. Aqua MODIS C7 electronic crosstalk correction coefficients mission-long trends.

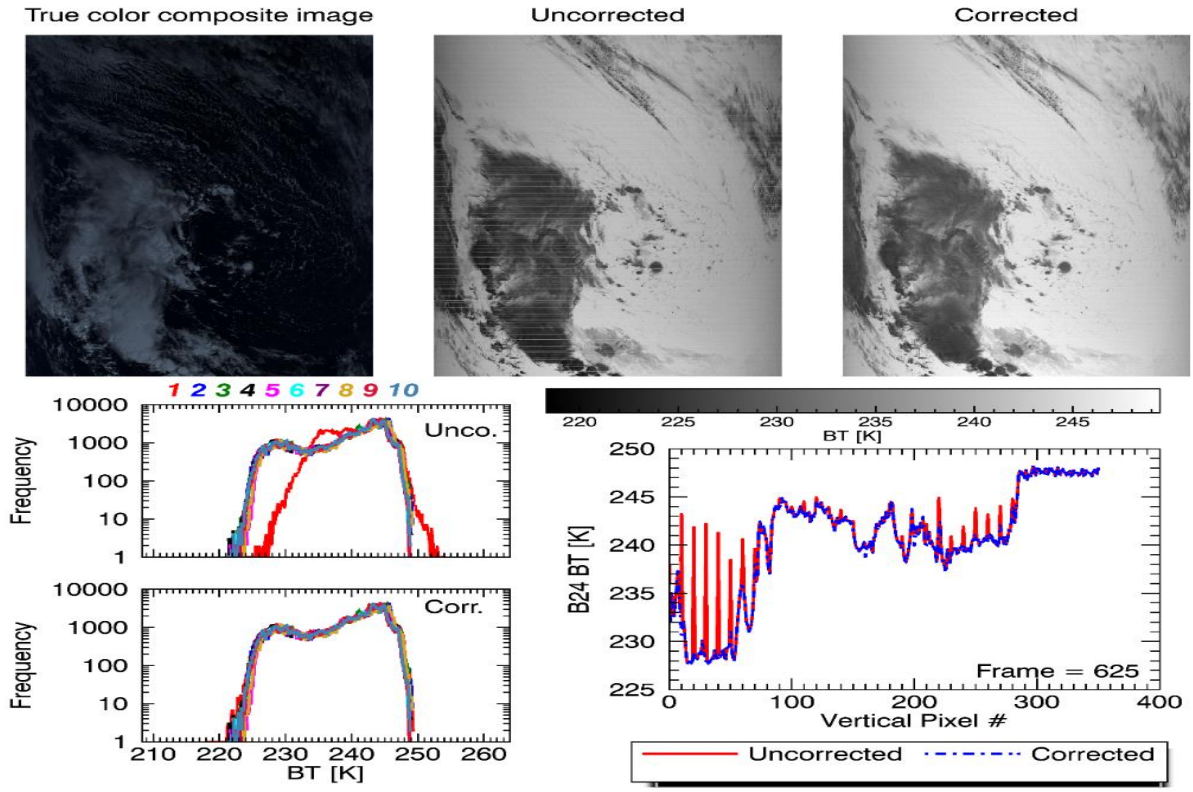

Figure 10. Electronic crosstalk correction coefficients application on the L1B product example for Aqua MODIS band 24, detector 1 (P.O.). The L1B images displayed correspond to a granule from October 11th, 2019.

4.1.2 PV LWIR electronic crosstalk correction

As presented in section 2.2, two types of crosstalk contaminate the MODIS TEB PV LWIR bands. One is detector-to-detector, normally the sending signal is from detector 10 from another band and the receiver is detector 1. The second type is from band-to-band between the PV LWIR bands. For Aqua, the detector-to-detector contamination is large at the mission beginning and decreases with time. The band-to-band contamination increases with time. Figure 11 shows Aqua MODIS electronic crosstalk correction coefficients mission-long trends for band 30. These crosstalk coefficients are derived from lunar observations. Bands 27 and 29 have similar patterns of the trending while band 28 crosstalk is insignificant. Two types of crosstalk coefficients are shown: detector 1 crosstalk from band 29 detector 10 and the crosstalk from the four PV LWIR bands. The detector 1 crosstalk from band 29 detector 10 is around 3.7% in the mission beginning down to 2.5%. The band-to-band crosstalk shows the trending is increasing in absolute value.

Based on the observable contamination for the PV LWIR bands' detector 1, the correction is applied for C7. The band-to-band contamination is the summation of all the sending detectors of the four sending bands. Its contamination is significant and shows an increasing trend. The contamination affects the trending of the Earth measurement of the entire band and L1B product quality. After evaluation and tests, the band-to-band crosstalk for bands 27, 29, and 30 are also corrected for C7.

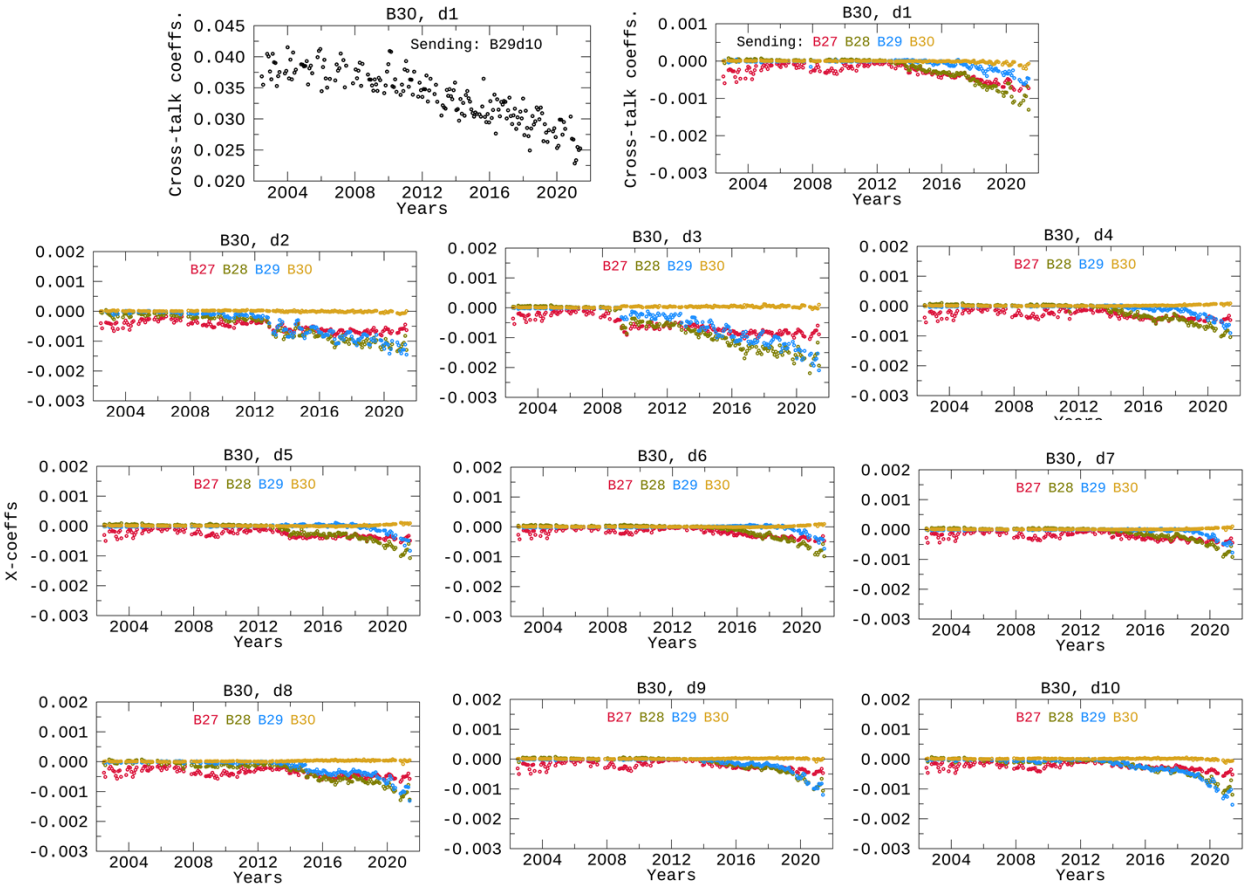

Figure 11. Aqua MODIS electronic crosstalk correction coefficients mission-long trends for band 30. For detector 1, two types of crosstalk coefficients are shown on the top. The left chart shows the trending of the detector 1 crosstalk from band 29 detector 10, and the right chart shows the crosstalk from the four PV LWIR bands. The charts below are for the band-to-band crosstalk for detectors 2 to 10.

4.2 Nonlinear coefficient calibration improvement

4.2.1 Mirror side difference correction

As shown in Table 2 for C6.1, the pre-launch a_0 with instrument temperature adjustment is used for Aqua PV bands 20-25 and 27-30, while a_0 is set to zero for PC bands 31-36. After the Aqua MODIS mission-long mirror side BT differences were analyzed using qDCC, the formatter reset event (January 2018) was found to have caused significant changes in the mirror side difference. The method was applied to all the MODIS TEB (except bands 21 and 31 because…..?). Figure 12 illustrates the Aqua MODIS mission-long mirror side BT differences for select bands. Band 20 has the largest mirror side BT difference (approximately 1.8 K) before the formatter reset. After the reset, this mirror side difference is reduced (decreased to 0.5 K). The other MWIR TEB also show up to a 1 K mirror side BT difference before the formatter reset event. Because band 21 uses a linear calibration algorithm with a_0 and a_2 set to zero, its mirror side BT differences are not directly comparable to the other bands. Figure 12 shows the mirror side difference for band 20 and 24, and the other bands have similar patterns. For all MWIR bands, the mirror side differences are smaller after the reset. A more detailed description of the MODIS TEB calibration algorithm improvements for C7 is provided by Chang et al.[23].

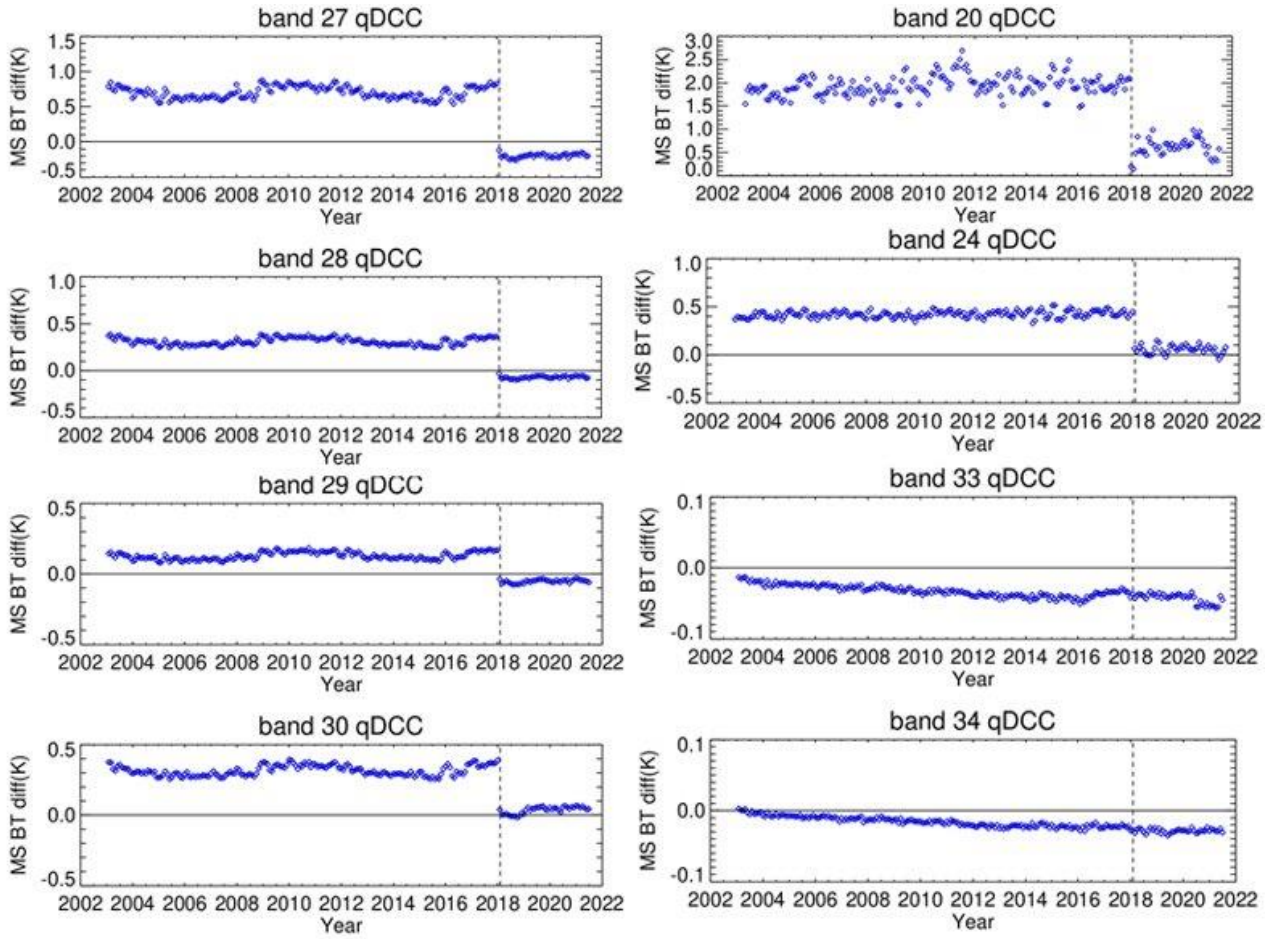

Figure 12. Aqua long-term mirror side BT differences over qDCC using C6.1. Each symbol represents monthly-averaged mirror side differences. The vertical dashed line indicates the time of occurrence for the formatter reset (January 2018).

The left panel of Figure 12 shows the Aqua MODIS mission-long mirror side BT differences for the PV LWIR bands 27-30. Band 27 has the largest mirror side difference among these four bands (approximately 0.8 K) before the formatter reset. Similar to the MWIR TEB, after the reset, the mirror side differences for all four bands decreased significantly. Moreover, all four bands exhibit slight - and similar in pattern – fluctuations in the mirror side difference. The PC LWIR TEB mirror side differences are small and not shown here. Amission-long a_0 correction for all TEB have been processed with the C7 LUT- except for bands 21 and 31. Only a linear calibration is applied to band 21 in C7, and thus the a_0 correction is not applied to this band. Band 31 is used as the reference band for the qDCC pixel identification process; hence no mirror side differences and no a_0 corrections are derived for this band. Moreover, band 31 exhibits accurate calibration and excellent stability. As such, its mirror side differences are expected to be negligible. For PC bands, the mirror side differences are insignificant, and the formatter reset does not have significant impact. The right panel of Figure 12 shows bands 33 and 34 for illustration and the other PC bands show a similar behavior.

After deriving the a_0 bias correction using extremely cold scenes (i.e. qDCC), a set of test LUTs (later on referred to as C7) were developed to evaluate their efficacy in reducing the Aqua MODIS TEB mirror side differences when compared to C6.1. The C7 algorithm was slightly changed to the one currently employed in C6.1 by applying the derived bias correction to the pre-launch a_0 coefficients and, the a_2 coefficients are derived using the CD data from each WUCD operation. There was no algorithm change to the band 21 b_1 coefficients (linear fit with a_0 and a_2 equal to zero). Using C7 LUTs, selected EV targets were evaluated by producing C7 test L1B data to compare with the official C6.1 L1B product. The test results demonstrate significant reduction in mirror side differences for all TEB.

4.2.2 PV LWIR bands stability improvement

Similar with Terra, Aqua PV LWIR bands have crosstalk and long-term stability issues. The Aqua-IASI comparisons and measurements trending over the Ocean, desert, Dome-C, and qDCC are used for long-term stability assessment. It is found that the long-term stability is BT dependent. Over the entire mission, band 29 shows upward trend (include magnitude here). Band 30 shows the largest drift and majority of the drift is from 2012 to 2021. Bands 27 and 28 show a similar pattern as band 30 with smaller drift. For C6.1, the rate of change is up to 0.67K/year for these bands. A similar method as Terra band 30 is applied to the Aqua PV LWIR bands. The C7 calibration algorithm improvements for these bands include crosstalk correction and the a_2 LUT remains the same after 2012-036. For band 27, 28, and 30, these calibration improvements largely reduce the drift. For band 29, after application of the crosstalk correction and the a_2 algorithm, the trending assessments of measurements over Earth scenes show the improvements over warm scene such as ocean and desert. However, the Dome-C trending shows 0.5 K drift over the mission. Additional a_0 correction based on Dome-C drift is used to improve the trending at low BT Earth scenes for band 29. Table 5 lists the change rate in C6.1 and C7 after calibration improvements. Due to the coupling of the a_0 and a_2 effects on the measurement, the improvement is BT dependent.

Table 5. Aqua MODIS PV LWIR bands change rate from long-term measurements over Dome-C, desert, and ocean, for C6.1 and C7. The average BT is in K and the change rate is in K/year. The negative sign means downward drift and positive sign means upward drift.

Scene	Band	Scene BT (K)	C6.1 MS diff. (K/yr)	C7 MS diff. (K/yr)
Dome-C	27	224	-0.59	-0.21
	28	221	-0.34	-0.09
	29	218	0.22	0.10
	30	220	-0.41	0.23
Desert	27	250	-0.62	-0.02
	28	264	-0.08	0.09
	29	279	0.67	0.39
	30	266	-0.41	0.02
Ocean	27	248	-0.53	0.06
	28	264	-0.16	0.01
	29	291	0.34	0.20
	30	274	-0.40	-0.01

4.2.3 Impact assessment

Similar to section 3.2.4 for Terra C7, impact assessment of the calibration algorithm improvement on the L1B product uses simulated L1A data. Table 6 lists the impact at three radiance levels for years 2005, 2015, and 2020. This assessment is also for the band average. As expected, the largest change observed is for band 30, which is up to 1.5K for the most recent year. The band 30 change is also time dependent since the major C7 improvement is the mitigation of its downward

trend. Band 29 C7 calibration improvements also have impact up to 1.4K for the maximum radiance level and 0.4 for typical and low radiance levels for recent years, and the changes in early mission are small for this radiance range. The mirror side difference correction presented in section 4.2.1 does not have much impact on the band averaged assessment. The improvements for low BT scene are below this assessment range and the impact of the calibration algorithm change is small. The calibration algorithm changes for the nonlinear coefficients also have impact less than 0.4K.

Table 6. Aqua MODIS TEB C7 impact assessments calculated as the BT difference between C7 and C6.1 in Kevin

Year	2005			2015			2020		
Radiance level	0.3Ltyp	Ltyp	Lmax	0.3Ltyp	Ltyp	Lmax	0.3Ltyp	Ltyp	Lmax
20	0.018	-0.053	-0.433	0.018	-0.052	-0.425	0.017	-0.048	-0.394
21	0.365	0.405	0.820	-0.187	-0.261	-0.170	0.000	0.000	0.000
22	0.022	-0.056	-0.325	0.022	-0.056	-0.321	0.022	-0.055	-0.318
23	0.024	-0.055	-0.321	0.022	-0.056	-0.306	0.022	-0.054	-0.301
24	0.039	0.014	0.016	0.004	0.030	0.016	0.021	0.022	0.017
25	0.015	0.009	0.000	0.014	0.007	0.000	0.014	0.009	0.000
27	-0.056	-0.007	-0.005	0.066	0.052	0.029	0.282	0.298	0.160
28	0.033	0.034	0.015	0.109	0.087	0.035	0.345	0.304	0.131
29	0.046	-0.029	-0.121	0.048	-0.103	-0.393	0.380	-0.372	-1.366
30	0.077	0.079	0.033	0.361	0.310	0.128	1.518	1.267	0.464
31	-0.004	0.003	0.008	-0.004	0.002	0.008	0.002	-0.001	-0.003
32	-0.008	0.005	0.013	-0.006	0.004	0.011	0.002	-0.001	-0.003
33	-0.375	-0.225	-0.002	-0.374	-0.222	0.000	-0.376	-0.224	-0.003
34	-0.098	-0.073	-0.043	-0.112	-0.089	-0.048	-0.102	-0.076	-0.046
35	-0.327	-0.280	-0.186	-0.353	-0.300	-0.199	-0.350	-0.302	-0.197
36	-0.215	-0.174	-0.161	-0.260	-0.225	-0.205	-0.248	-0.298	-0.199

4.2.4 Uncertainty update

The calibration uncertainties propagate to the total uncertainty of the L1B product. Similar to Terra, the uncertainty is updated for C7. The crosstalk contamination of the selected detectors and bands are also included for the uncertainty using a penalty LUT. Figure 13 shows the total uncertainty without EV noise and crosstalk effect for TEB for selected years for C6.1 and C7. Aqua MODIS TEB calibration coefficients are more stable than Terra and the crosstalk contaminations are also less than Terra. The uncertainties for C6.1 and for C7 are comparable.

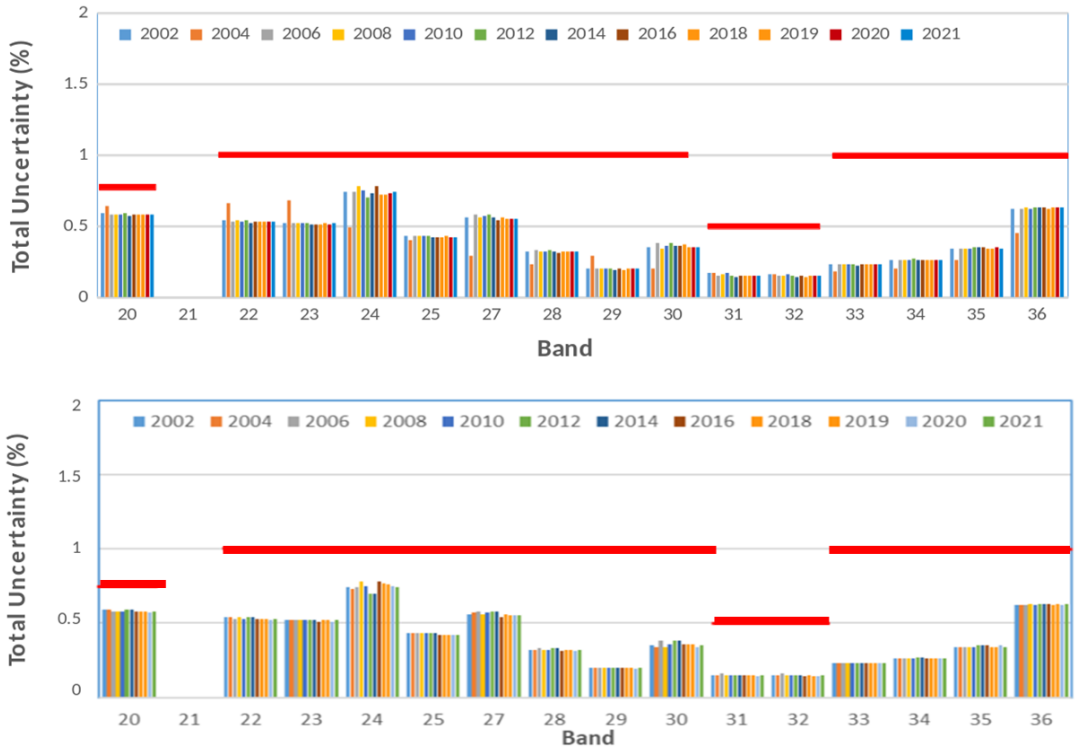

Figure 13. (Top) Aqua MODIS TEB C6.1 uncertainty for selected years. (Bottom) Aqua MODIS TEB C7 uncertainty for selected years. The red horizontal lines are the specifications.

6. SUMMARY

After more than 21 and 19 years on-orbit, the Terra and Aqua MODIS TEB performance has been generally stable. However, contamination from electronic crosstalk affects the L1B image quality and measurement accuracy. The instrument nonlinear calibration uncertainty also affects the calibration and measurement stability. Several calibration algorithm improvements were discussed, tested, validated, and are hereby implemented by MCST for C7. The calibration algorithm improvements are based on a thorough review of the C6.1 TEB LUT algorithm, and calibration assessments using Earth scenes and sensor inter-comparisons. The Earth measurement assessments show that the major instrument configuration changes affect the instrument nonlinear response and crosstalk, and the expected improvement in image quality, measurement stability and consistency.

ACKNOWLEDGMENTS

The authors would like to acknowledge Amit Angal for internal reviews of this paper, and discussions with Chris Moeller and other MODIS science teams.

REFERENCES

[1] Barnes, W. L. and V. V. Salomonson, “MODIS: A global image spectroradiometer for the Earth Observing System,” Crit. Rev. Opt. Sci. Technol., vol. CR47, 285–307, 1993.

[2] Barnes, W. L.,V. V. Salomonson, B. Guenther, and X. Xiong, “Development, characterization, and performance of the EOS MODIS sensors,” in Proc. SPIE, 5151, 337–345, 2003.
[3] Barnes, W. L., X. Xiong, and V. V. Salomonson, “Status of Terra MODIS and Aqua MODIS,” J. Adv. Space Res., 32(11), 2099–2106, 2003.
[4] Salomonson, V. V., W. L. Barnes, X. Xiong, S. Kempler, and E. Masuoka, “An overview of the Earth Observing System MODIS instrument and associated data systems performance,” in Proc. IEEE IGARSS, 1174–1176, 2002.
[5] Parkinson, C. L., "Summarizing the first ten years of NASA's Aqua mission", IEEE J. Sel. Topics Appl. Earth Observ. Remote Sens., 6(3), 1179-1188, 2013.
[6] Yue, H., C. He, Y. Zhao, Q. Ma; Q. Zhang, “The brightness temperature adjusted dust index: An improved approach to detect dust storms using MODIS imagery”. INTERNATIONAL JOURNAL OF APPLIED EARTH OBSERVATION AND GEOINFORMATION, 57, 166-176, 2017.
[7] Skakun, S., CO Justice, E Vermote, JC Roger Transitioning from MODIS to VIIRS: an analysis of inter-consistency of NDVI data sets for agricultural monitoring” International journal of remote sensing, 39(4), 971-992, 2018
[8] Gupta, P., L. A. Remer, R. C. Levy, and S. Mattoo, “Validation of MODIS 3 km land aerosol optical depth from NASA's EOS Terra and Aqua missions” Atmospheric Measurement Techniques; Katlenburg-Lindau 11 (5), 2018
[9] Levy, R. C., S. Mattoo, L. A. Munchak, L. A. Remer, A. M. Sayer, F. Patadia, and N. C. Hsu, “The Collection 6 MODIS aerosol products over land and ocean”, Atmos. Meas. Tech., 6, 2989–3034, 2013
[10] Sun, J., X. Xiong, Y. Li, S. Madhavan, A. Wu, and B. N. Wenny, "Evaluation of Radiometric Improvements With Electronic Crosstalk Correction for Terra MODIS Band 27", IEEE Transactions on Geoscience and Remote Sensing, vol. 52, issue 10, pp. 6497 - 6507, 2014.
[11] Wilson, T., A. Wu, A. Shrestha, X. Geng, Z. Wang, C. Moeller, R. Frey, and X. Xiong, "Development and Implementation of an Electronic Crosstalk Correction for Bands 27–30 in Terra MODIS Collection 6,” Remote Sens., vol. 9, issue 569, 2017.
[12] Xiong, X., A. Wu, B. N. Wenny, S. Madhavan, Z. Wang, Y. Li, N. Chen, W. Barnes, and V. Salomonson, "Terra and Aqua MODIS Thermal Emissive Bands On-Orbit Calibration and Performance", IEEE Transactions on Geoscience and Remote Sensing, vol. 53, issue 10, pp. 5709 - 5721, 2015.
[13] MODIS Thermal Emissive Band Crosstalk Workshop. MsWG meeting. August 2018. https://mcst.gsfc.nasa.gov/meetings/modis-thermal-emissive-band-crosstalk-workshop.
[14] Wu, A., Z. Wang, Y. Li, S. Madhavan, B. N. Wenny, N. Chen, and X. Xiong, "Adjusting Aqua MODIS TEB nonlinear calibration coefficients using iterative solution," Proc. SPIE 9264, Earth Observing Missions and Sensors: Development, Implementation, and Characterization III, 92640R (2 December 2014); https://doi.org/10.1117/12.2069246.
[15] Moeller, C. MODIS and VIIRS TEB Performance. MCST and VCST Calibration Workshop 2019. November 2019. https://mcst.gsfc.nasa.gov/sites/default/files/meetings_files/03_Moeller_TEBVIIRS.pdf
[16] Li Y., A. Wu, and X. Xiong, "Assessment of MODIS collection 6.1 thermal emissive band calibration using hyperspectral IASI observations," Proc. SPIE 11530, Sensors, Systems, and Next-Generation Satellites XXIV, 1153019 (20 September 2020); https://doi.org/10.1117/12.2571488.
[17] Chang, T., X. Xiong, and A. Angal, "Terra and Aqua MODIS TEB intercomparison using Himawari-8/AHI as reference", Journal of Applied Remote Sensing, vol. 13, issue 1, pp. 017501, 2019.
[18] Pérez Díaz, C., X. Xiong, and A. Wu, "MODIS thermal emissive bands calibration stability using in-situ ocean targets and remotely-sensed SST retrievals provided by the group for high resolution sea surface temperature," Proc. SPIE 11014, Ocean Sensing and Monitoring XI, 110140P (10 May 2019); https://doi.org/10.1117/12.2518691.
[19] Xiong, X., A. Shrestha, and B. Wenny, "Assessments of MODIS thermal emissive bands on-orbit calibration performance using Dome C observations," Proc. SPIE 10986, Algorithms, Technologies, and Applications for Multispectral and Hyperspectral Imagery XXV, 1098605 (14 May 2019); https://doi.org/10.1117/12.2519000.
[20] Xiong, X., A. Angal, W. L. Barnes, H. Chen, V. Chiang, X. Geng, Y. Li, K. Twedt, Z. Wang, T. Wilson, et al., "Updates of Moderate Resolution Imaging Spectroradiometer on-orbit calibration uncertainty assessments", Journal of Applied Remote Sensing, vol. 12(3),034001, 2018.
[21] Keller, G. R., Z. Wang, A. Wu, and X. Xiong, "Aqua MODIS electronic crosstalk survey from Moon observations," Proc. SPIE 10423, Sensors, Systems, and Next-Generation Satellites XXI, 1042314 (29 September 2017); https://doi.org/10.1117/12.2277972.
[22] Keller, G. R., T. Wilson, X. Geng, A. Wu, Z. Wang and X. Xiong, "Aqua MODIS Electronic Crosstalk Survey: Mid-Wave Infrared Bands," IEEE Transactions on Geoscience and Remote Sensing, vol. 57, no. 3, pp. 1684-1697, 2019, doi: 10.1109/TGRS.2018.2868613.

[23] Chang, T., X. Xiong, A. Shrestha, and C. Perez Diaz, “Methodology development for calibration assessment using quasi-deep convective clouds with application to Aqua MODIS TEB. Earth and Space Science,” vol. 7, e2019EA001055, 2020. https://doi.org/10.1029/2019EA001055